THE EIGENVALUE SPECTRUM OF LAGGED CORRELATION MATRICES*

Stefan Thurner[a,b], Christoly Biely[a]

[a]Complex Systems Research Group, HNO, Medical University of Vienna
Währinger Gürtel 18-20, A–1090 Vienna, Austria

[b]Santa Fe Institute
1399 Hyde Park Road, Santa Fe, NM 87501, USA

(Received October 1, 2007)

We derive the exact form of the eigenvalue spectrum of correlation matrices obtained from a set of N time-shifted, iid Gaussian time-series of length T. These matrices are random, real and asymmetric matrices with a superimposed structure due to the time-lag. We demonstrate that the associated (complex) eigenvalue spectrum is circular symmetric for large matrices ($\lim N \to \infty$). This fact allows to exactly compute the eigenvalue density via the inverse Abel-transform of the density of the *symmetrized* problem. The validity of the approach is demonstrated by comparison to numerical realizations of random time-series. As an example, spectra of correlation matrices from time-lagged financial data are presented.

PACS numbers: 02.50.–r, 02.10.Yn, 05.40.–a, 87.10.+e

1. Introduction

In its simplest form, a random matrix ensemble is an ensemble of $N \times N$ matrices $\boldsymbol{M}$ whose entries M_{ij} are uncorrelated iid random variables, and whose distribution is given by

$$P(\boldsymbol{M}) \sim \exp\left(-\frac{\beta N}{2}\mathrm{Tr}\ \boldsymbol{M}\boldsymbol{M}^T\right), \tag{1}$$

where β takes specific values for different ensembles of matrices (*e.g.* depending on whether the random variables are complex- or real-valued). Eigenvalue spectra and correlations of eigenvalues in the limit $N \to \infty$ have been

* Presented at the Conference on Random Matrix Theory, "From Fundamental Physics to Applications", Kraków, Poland, May 2–6, 2007.

worked out for *symmetric* $N \times N$ random matrices by Wigner [1]. For real valued matrix entries, such symmetric random matrices are referred to as the Gaussian orthogonal ensemble (GOE). The symmetry constraint has later been relaxed by Ginibre and the probability distributions of different ensembles (real, complex, quaternion) — known as Ginibre ensembles (GinOE, GinUE, GinSE) — have been derived [2] in the limit of infinite matrix size. For ensembles of random, real asymmetric matrices (GinOE) — the most difficult case — progress has been slow despite the great efforts undertaken in the past decades. The eigenvalue density could finally be derived via different methods [3, 4], where — quite remarkably — the finite-size dependence of the ensemble has also been understood [4]. For recent progress in the field see [5].

However, these developments in random matrix theory (RMT) cannot be used for (lagged) correlation matrices obtained from finite rectangular $N \times T$ matrices $\boldsymbol{X}$, which contain N time-series of length T. The matrix ensemble corresponding to the $N \times N$ covariance matrix $\boldsymbol{C} \sim \boldsymbol{X}\boldsymbol{X}^T$ is known as the Wishart ensemble [6] and is a cornerstone of multivariate data analysis. For the case of uncorrelated Gaussian distributed data, the exact solution to the eigenvalue-spectrum of $\boldsymbol{X}\boldsymbol{X}^T$ is known as the Marcenko–Pastur law for $N \to \infty$. The time-lagged analogon to the covariance matrix is defined as $C_\tau^{ij} \sim \sum_t^T x_t^i x_{t-\tau}^j$, where one time-series x_t^i is shifted by τ timesteps with respect to the other. In contrast to (real-valued) equal-time correlation matrices of the Wishart ensemble, the spectrum of $\boldsymbol{C}_\tau$ is in general complex. While the complex spectrum of $\boldsymbol{C}_\tau$ remains unknown so far, results for *symmetrized* lagged correlation matrices have been reported recently [7, 8]. In [8], it was also shown that the methodology of free random variables can be used to tackle a variety of correlated (symmetric) Wishart matrix models. However, it is the analysis of the asymmetric time-lagged correlations which would be highly desirable for many applications, which involve non-trivial lead-lag relationships, ranging from finance and econometrics to biology and physics. Here we review the methodology for the eigenvalue analysis of such time-lagged correlations [9]. In Section 2 we discuss how solutions of RMT problems pertaining to real, asymmetric matrices can be exactly obtained from solutions to the symmetrized problem via the inverse Abel-transform. This allows to derive the eigenvalue spectra. As an example we compare the theoretical results with real financial data in Section 3, and conclude in Section 4.

2. Spectra of time-lagged correlation matrices

The entries in the $N \times T$ data matrices $\boldsymbol{X}$ for N time-series of length T are denoted by x_t^i, which are Gaussian iid random variables. Time-lagged correlations are defined as

$$C_\tau^{ij} \equiv \frac{\left\langle \left(x_t^i - \left\langle x_t^i \right\rangle \right) \left(x_{t-\tau}^j - \left\langle x_{t-\tau}^j \right\rangle \right) \right\rangle}{\sigma_i \sigma_j} , \tag{2}$$

where τ is the time-lag and σ_i is the standard deviation of time-series i. For $\tau \neq 0$, the lagged correlation matrix $\boldsymbol{C}_\tau$ is generally not symmetric and can be written as

$$\boldsymbol{C}_\tau = \frac{1}{T} \boldsymbol{X} \boldsymbol{D}_\tau \boldsymbol{X}^{\boldsymbol{T}} , \tag{3}$$

where $\boldsymbol{D}_\tau \equiv \delta_{t,t+\tau}$. Denoting the eigenvalues of C_τ^{ij} by λ_i and their associated eigenvectors by $\vec{u}_i$, the eigenvalue problem is

$$\sum_j C_\tau^{ij} \vec{u}_j = \lambda_j \vec{u}_j . \tag{4}$$

Eigenvalues λ_i are either real or complex conjugate (for real C_τ^{ij} the conjugate eigenvalue λ_i^* also solves Eq. (4)). Regarding the elements of C_τ^{ij} as random variables note that their specific construction, Eq. (3), results in a departure from real, asymmetric $N \times N$ matrix with iid Gaussian entries. Unfortunately, powerful addition formalisms developed for non-Hermitian random matrices (see *e.g.* [10] and references therein) are not applicable in the case of random real asymmetric matrices. However, it was shown that the problem can be treated in a way formally equivalent to classical electrostatics [3, 11] and a generalization of Girko's semicircular law [12] could be recovered with the replica technique.

2.1. The general argument

We start our argument from the electrostatic potential analogy introduced by Wigner. The idea is to interpret the distribution of eigenvalues in the complex plane as a distribution of electrical charges in two dimensions. Following the same arguments as in [11], the corresponding potential is

$$\phi(x,y) = -\frac{1}{N} \left\langle \ln \det \left(\left(\delta_{ij} z^* - C_\tau^{ji} \right) \left(\delta_{ij} z - C_\tau^{ij} \right) \right) \right\rangle_c , \tag{5}$$

where $z = x + iy$, and $\langle ... \rangle_c$ denotes the average over the distribution,

$$P(\boldsymbol{X}) \sim \exp \left(-\frac{N}{2} \mathrm{Tr}\ \boldsymbol{X} \boldsymbol{X}^{\boldsymbol{T}} \right) . \tag{6}$$

It can be shown [11] that Eq. (5) allows for the calculation of a density $\rho(z) = \rho(x,y)$ via the Poisson equation

$$\rho(x,y) = -\frac{1}{4\pi} \triangle \phi(x,y) . \tag{7}$$

Expanding the argument of the determinant in Eq. (5) we obtain the positive definite matrix

$$H_{ij} = \delta_{ij}|z| + C_\tau^{ij}C_\tau^{ji} - x\left(C_\tau^{ij} + C_\tau^{ji}\right) + iy\left(C_\tau^{ij} - C_\tau^{ji}\right) . \tag{8}$$

This form shows that any symmetric (anti-symmetric) contribution of C_τ^{ij} only influences the real (imaginary) part of z. If there is no structural difference in randomness for the symmetric and the anti-symmetric part of matrix $\boldsymbol{C}_\tau$, the expression of Eq. (8) is equivalent under exchange of x and y (distribution sense), and Eq. (7) is symmetric in x and y. Since we do not expect any direction in the complex plane being distinguished from any other in the limit $N \to \infty$, we conceive that the eigenvalue density resulting from Eq. (5) is a radially symmetric function, *i.e.*,

$$\rho(x,y) = \rho(r) \equiv \frac{1}{2\pi r}\int\limits_{\mathcal{S}} dz\rho(z)\,\delta(|z| - r)\,. \tag{9}$$

A more formal argument can be given by expanding H_{ij} entering the potential ϕ [13]. Since typically $C_{ij} < 1$, one can write $H_{ij} \approx |z|(A + \varepsilon B)$, where ε is a small perturbation, $A = \delta_{ij}$ and $B = C^{ij}C^{ji}/|z| - \bar{x}\left(C^{ij} - C^{ji}\right) + i\bar{y}\left(C^{ij} + C^{ji}\right)$ with $\bar{x} = x/|z|$ and $\bar{y} = y/|z|$. Without loss of generality we can fix $|z| = 1$ and expand the determinant,

$$\begin{aligned}\phi(x,y) &= -\frac{1}{N}\langle \ln\det(H_{ij})\rangle_c = -\frac{1}{N}\langle \mathrm{Tr}\ln(H_{ij})\rangle_c \\ &\approx -\frac{1}{N}\left\langle \mathrm{Tr}(B) - \mathrm{Tr}\left(\frac{B^2}{2}\right) + \mathrm{Tr}\left(\frac{B^3}{3}\right) - \cdots\right\rangle_c .\end{aligned} \tag{10}$$

We checked to fourth order that this expansion indeed only leads to terms in r for $N \to \infty$, [9]. A more direct way of proving the conjecture would be to replace the determinant in Eq. (5) by Gaussian integrals and use the replica method to average over the distribution of the C_{ij}.

If $\rho(r)$ is circular symmetric, the support $\mathcal{S}$ of the eigenvalue-spectrum will be bounded by a circle with radius $r_{\max}$. Since $r_{\max}$ is governed by the standard deviation of the underlying random matrix elements, one can compute the extent of the support of $\boldsymbol{C}_\tau$ by considering the support of the symmetric ($r_{\max}^{\mathrm{S}}$) and the anti-symmetric matrices ($r_{\max}^{\mathrm{A}}$), defined by $\boldsymbol{C}_\tau^{\mathrm{S}} \equiv \frac{1}{2}(\boldsymbol{C}_\tau + \boldsymbol{C}_\tau{}^T)$ and $\boldsymbol{C}_\tau^{\mathrm{A}} \equiv \frac{1}{2}(\boldsymbol{C}_\tau - \boldsymbol{C}_\tau{}^T)$. Assuming equal standard deviations of the symmetric and anti-symmetric matrices, $\sigma_{\mathrm{S}} = \sigma_{\mathrm{A}}$, implies that the standard deviation σ of matrix C_τ^{ij}, is $\sigma = \sqrt{2}\sigma_{\mathrm{S}}/2$. Thus, the support of $\boldsymbol{C}_\tau$ is naturally defined by the disc of radius

$$r_{\max}^{\mathcal{S}} = \frac{1}{\sqrt{2}}r_{\max}^{\mathrm{S}} = \frac{1}{\sqrt{2}}r_{\max}^{\mathrm{A}}\,. \tag{11}$$

The argument here is that the eigenvalue-density can be regarded as a 'log-gas' [14] which has only one degree of freedom for $\boldsymbol{C}_\tau^{\mathrm{S}}$ and $\boldsymbol{C}_\tau^{\mathrm{A}}$, but two degrees of freedom for $\boldsymbol{C}_\tau$, hence leading to $\sigma = \sqrt{2}\sigma_{\mathrm{S}}/2$ instead of $\sqrt{2}\sigma_{\mathrm{S}}$.

Based on these relations and the discussion of Eq. (8), it is sensible to conjecture that the projections of $\rho(r)$ onto the x-axis, denoted by $\rho_x(\lambda)$, and the projection onto the y-axis, $\rho_y(\lambda)$, are nothing but the rescaled spectra of the solution to the symmetric, $\rho^{\mathrm{S}}(\lambda)$, and to the anti-symmetric problem, $\rho^{\mathrm{A}}(y)$. To be more explicit,

$$\begin{aligned}\rho_x(\lambda) \equiv \rho(\mathrm{Re}(\lambda)) &= \int\limits_{\mathcal{S}} dy\, \rho(r) = \rho^{\mathrm{S}}\left(\sqrt{2}x\right)\,, \\ \rho_y(\lambda) \equiv \rho(\mathrm{Im}(\lambda)) &= \int\limits_{\mathcal{S}} dx\, \rho(r) = \rho^{\mathrm{A}}\left(\sqrt{2}y\right)\,, \end{aligned} \tag{12}$$

where integration extends over the support $\mathcal{S}$ in the complex plane. Although this conjecture might seem quite natural we shall provide numerical evidence for its correctness below.

The eigenvalue density of the symmetric problem can be obtained from the well-known relation

$$\rho^{\mathrm{S}}(x) = \sum_n \delta(x - x_n) = \frac{1}{\pi} \lim_{\varepsilon \to 0} \left[\mathrm{Im}\left(G^{\mathrm{S}}\left(x - i\varepsilon\right)\right)\right]\,. \tag{13}$$

For radial symmetry of course, $\rho^{\mathrm{S}} \sim \rho^{\mathrm{A}}$. The main idea is to use the following method to determine the radially symmetric density $\rho(r)$: Since the rescaled eigenvalue density of the symmetrized problem $\rho^{\mathrm{S}}\left(\sqrt{2}x\right)$ is nothing but the projection of $\rho(r)$ onto the real axis, Eq. (12), it can be written as the Abel-transform [15] of the radial density $\rho(r)$,

$$\rho^{\mathrm{S}}\left(\sqrt{2}x\right) = 2\int\limits_x^\infty dr\, \frac{\rho(r) r}{\sqrt{r^2 - x^2}}\,. \tag{14}$$

One can then reconstruct the eigenvalue spectrum *exactly* (in the limit $N \to \infty$) via the inverse Abel-transform, and thus via the cuts of the Greens function of the symmetric problem,

$$\rho(r) = -\frac{1}{\pi^2} \int\limits_r^\infty \frac{\frac{d}{dx} \lim_{\varepsilon \to 0} \left[\mathrm{Im}\left(G_\tau^{\mathrm{S}}\left(\sqrt{2}x - i\varepsilon\right)\right)\right]}{\sqrt{x^2 - r^2}}\, dx\,, \tag{15}$$

where we have made use of Eq. (13). Typically, the solution of the symmetric problem is valid in the $N \to \infty$ limit; finite-size effects in real data might cause deviations from the exact result.

As an example the uniform eigenvalue distribution of real asymmetric matrices in the complex plane $\mathcal{C}$, found in [11], can be almost trivially recovered from Wigner's semicircle law of real symmetric matrices by applying the inverse Abel-transform. Starting from the semicircle law $\rho\left(\bar{\lambda}\right) = \frac{1}{2\pi}\sqrt{4-\bar{\lambda}^2}$ and after proper rescaling and normalization we insert $\rho^{\mathrm{S}}\left(\sqrt{2}x\right) = \frac{1}{\pi}\sqrt{2-x^2}$ into Eq. (15) to arrive at

$$\rho(r) = \frac{1}{\pi^2}\int_r^{\sqrt{2}} \frac{x}{\sqrt{2-x^2}\sqrt{x^2-r^2}}\mathrm{d}x = -\frac{1}{\pi^2}\arctan\left(\frac{\sqrt{2-x^2}}{\sqrt{x^2-r^2}}\right)\Bigg|_r^{\sqrt{2}} = \frac{1}{2\pi} \quad (16)$$

i.e., $\rho(r) = \frac{1}{2\pi}$ for $0 < r < \sqrt{2}$ and $\rho(r) = 0$ elsewhere.

2.2. Application to lagged correlation matrices

We now turn to the more specific problem of determining the eigenvalue density of $\boldsymbol{C}_\tau$. What is left is to confirm the validity of the conjecture, Eq. (12) and to show that — as a consequence — Eq. (15) gives the radial eigenvalue distribution, $\rho(r)$. We can refer to existing literature on the symmetric problem: It has been shown [7,8], that the Greens function, $G(z)$ of the symmetric problem, ${\boldsymbol{C}_\tau}^{\mathrm{S}} = \frac{1}{2T}\boldsymbol{X}(\boldsymbol{D}_\tau + \boldsymbol{D}_{-\tau})\boldsymbol{X}^T$, is given by

$$\frac{1}{Q^3}z^2G^4(z) - 2\frac{1}{Q^2}\left(\frac{1}{Q}-1\right)zG^3(z) - \frac{1}{Q}\left(z^2 - \left(\frac{1}{Q}-1\right)^2\right)G^2(z)$$
$$+2\left(\frac{1}{Q}-1\right)zG(z) + 2 - \frac{1}{Q} = 0\,, \quad (17)$$

with $Q \equiv T/N$ playing the role of a information-to-noise ratio. Note, that this equation is independent of a specific value for τ [8]. It is trivial to show that the Greens function pertaining to the anti-symmetric problem follows the same equation, which reaffirms circular symmetry. Based on Eq. (17) one can compute $\rho_x(\lambda)$ by using Eqs. (13) and (12).

Fig. 1 shows numerical realizations of spectra of $\boldsymbol{C}_{\tau=1}$ as defined in Eq. (3) with Gaussian iid entries in the columns of $\boldsymbol{X}$, for various values of Q. Note, that for $Q < 1$ the shape of the boundary of eigenvalues in the complex plane changes from a disk to an annulus (see *e.g.* [16] for a discussion of disc-annulus transition in non-hermitian matrix models). It is seen that eigenvalues are enhanced along the real axis which can be attributed to a well-known finite-size effect [3,11]. The prediction for the projections ρ_x and ρ_y (lines, obtained from Eq. (13) and Eq. (17) in Fig. 1) is in good agreement with the numerical data for the real parts of the eigenvalues (ρ_x). For the complex parts (ρ_y) we recognize that there is a slight deviation from the prediction due to the enhanced density along the real axis.

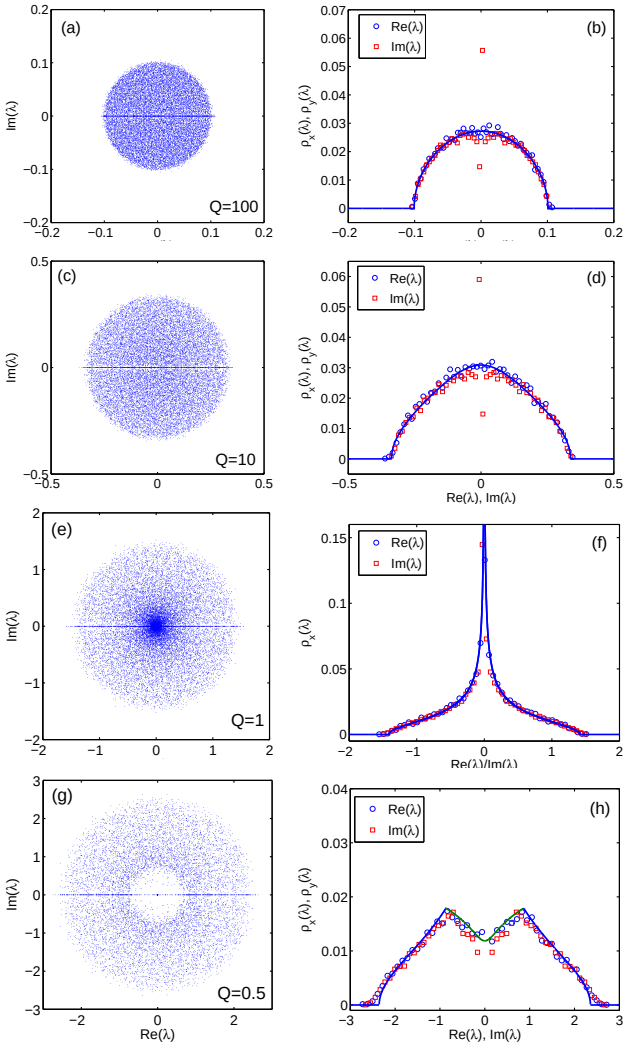

Fig. 1. Complex eigenvalue spectra of time-lagged correlation matrices, obtained from random matrices $\boldsymbol{X}$. The entries of $\boldsymbol{X}$ are iid and Gaussian with unit variance. In (a), (c), (e) and (g) the position of the eigenvalues is shown in the complex plane for values of $Q \equiv \frac{T}{N} = 100, 10, 1$ and 0.5, respectively. The visibly enhanced density along the real axis is the finite-size effect mentioned in the text. The right column shows the projections of the EVs onto the real and imaginary axis. Solid lines are the theoretical predictions (numerical solutions to Eq. (17)). Note in (h) that for this projection, the eigenvalue spectra is composed of different solutions to Eq. (17) as $G(z)$ itself has a discontinuity. The divergence at $z = 0$ is not shown for analytical curves associated with $Q = 100, 10$ and 0.5.

Finally, turning towards the point of reconstructing the radial eigenvalue density, the function to be transformed ($\rho^{\mathrm{S}}(\sqrt{2}x)$ or $\rho^{\mathrm{A}}(\sqrt{2}y)$) may be evaluated exactly (with some effort) for the symmetric case from Eq. (13) and Eq. (17). The remaining integral of Eq. (15) will, in general, be hard to solve. Nonetheless, we are able to solve it analytically for $Q = 1$ [9] and obtain the exact formula for the eigenvalue density,

$$\rho_{Q=1}(r) = \frac{1}{K}\left[2^{3/4}3r\Gamma\left(\frac{5}{4}\right)\Gamma\left(\frac{5}{4}\right)\Phi_2^1\left(\frac{1}{4},\frac{5}{4},\frac{3}{2},\frac{\lambda^2}{2}\right) - 2^{1/4}\Gamma\left(-\frac{1}{4}\right)\Gamma\left(\frac{7}{4}\right)\Phi_2^1\left(-\frac{1}{4},\frac{3}{4},\frac{1}{2},\frac{\lambda^2}{2}\right)\right], \tag{18}$$

with $K \equiv 6\sqrt{\pi^5 r^3}$. Here $\Gamma(x)$ is the Gamma- and $\Phi_2^1(a,b,c,z)$ the hypergeometric function. Note further that $\lim_{Q\to 0} G_Q^{\mathrm{S}}(z) = \frac{1}{z}$, whereas for $Q \to \infty$ the Greens function and the eigenvalue density converge to those of a random real, asymmetric matrix without specific structure, *i.e.* the flat eigenvalue density [11].

We were not able to derive closed expressions for other values of Q. In these cases the integral Eq. (15) has to be computed numerically. Results are shown in Fig. 2 for $Q = 100, 10$ and 1. The theoretical predictions are

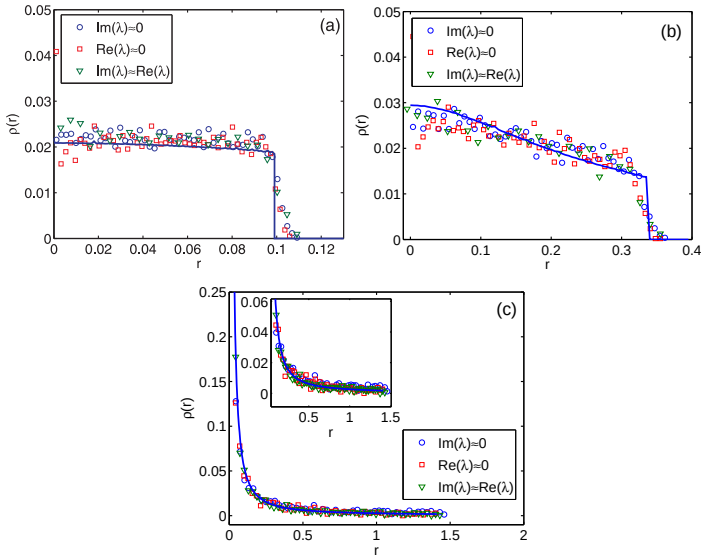

Fig. 2. Radial eigenvalue densities along different directions (real axis, imaginary axis and the diagonal in the complex plane. The solution of the inverse Abel-transform (lines) is compared with (finite) numerical data (symbols). (a) Q=100 (b) Q=10 (c) Q=1; the inset shows a detail of the curve.

compared to numerical data obtained from performing cuts along various directions of the spectra $\rho(x, y)$ from Fig. 1; along the x-axis, the y-axis and along the diagonal direction, *i.e.* $\mathrm{Re}(\lambda) = \mathrm{Im}(\lambda)$. These cuts were performed numerically by calculating the density within narrow ε-strips along the chosen directions. Again theoretical prediction and experimental densities coincide.

3. Empirical example of lagged financial data

RMT for equal-time covariance matrices has been extensively applied to financial data in the past years, see among many others *e.g.* [17–19]. Here we show results for the time-lagged case which could — so far — not be compared to theoretical results. In particular we analyze 5 min data of the S&P500 within the period of Jan. 2, 2002–Apr. 20, 2004. Time-series were cleaned, corrected for splits and synchronized. After cleaning, the data set $\boldsymbol{X}$ consisted of $N = 400$ log-return time-series of $T = 44720$ observations times each. Log-returns of asset i at observation times t are defined by

$$x_t^i \equiv \ln S_t^i - \ln S_{t-1}^i \,, \tag{19}$$

after subtraction of the mean and normalization to unit variance. S_t^i is the price of asset i at time t. The empirical time-series and their distribution-functions show the usual 'stylized facts' of high-frequency stock-returns (fat-tails, clustered volatility, equal-time correlation matrix element distribution, *etc.*).

Fig. 3 shows the eigenvalue spectrum obtained from $\boldsymbol{C}_1$ at various stages. In Fig. 3(a) a few deviations from the bulk of the eigenvalues are seen, most significantly one real eigenvalue $\lambda_1 \approx 4.6$ and a conjugate pair of complex eigenvalues at $\lambda_2 \approx 1.2$. Fig. 3(b) is a detail of (a) where a shift of the bulk of the eigenvalues with respect to the theoretical support (circle) is observed. This shift can be attributed to two effects: First, each deviating positive real eigenvalue $\tilde{\lambda}_i$ is associated with a shift s of the 'bulk' spectrum of $s \approx -\mathrm{Re}(\tilde{\lambda}_\mathrm{i})/N$ in direction of the negative real axis. ('Departing' eigenvalues are those which have real parts larger than the radius of the theoretical support.) The shift of the 'disc' pertaining to this effect is then the sum of all effects from departing eigenvalues, $s_\mathrm{tot} = -\frac{1}{N}\sum_{\tilde{\lambda}_i} \mathrm{Re}(\tilde{\lambda}_i) \approx -0.031$. The second contribution to the shift is due to the non-zero diagonal entries of the correlation matrices $\boldsymbol{C}_1$. The shift of the center of the disk explainable by the mean of the diagonal elements is $\bar{C}_1^{ii} = -0.029$, such that the overall displacement is $d = s_\mathrm{tot} + \bar{C}_1^{ii} = -0.060$. When corrected for the total shift one arrives at Fig. 3(c). The eigenvalues outside the theoretical regime should be associated with specific non-random structure present in the high-frequency return time-series. An in-depth analysis of the deviating eigenvalues and their meaning is presented in [9].

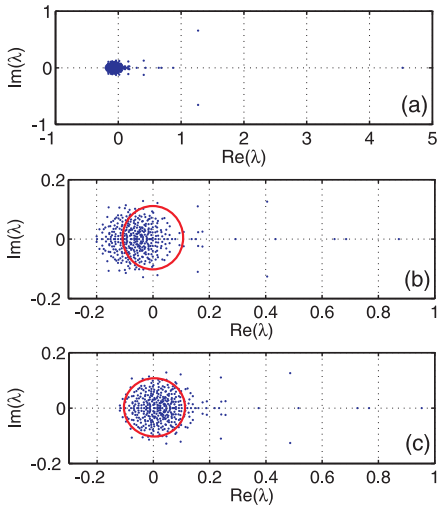

Fig. 3. Eigenvalue spectra of lagged correlation matrices from 5 min S&P500 data [9]. (a) shows the full spectrum with one very large deviation on the real axis ($\lambda_1 \sim 4.6$), and a large departing eigenvalue pair $\lambda_2 = \lambda_3^*$. (b) is a detail, clearly showing that the spectrum is shifted with respect to the 'bulk-disc'. (c) spectrum corrected for displacement d as discussed in the text. The circles in plots indicate the support discussed in Section 2.

Fig. 4 compares predictions from Section 2 with the projections of empirical eigenvalue data onto the real and imaginary axis. The inset shows the prediction of the radial density, integrated over the complex plane, $2r\pi\rho(r)$, compared with the empirical data, $\rho(|\lambda|)$. Empirical spectra are truncated

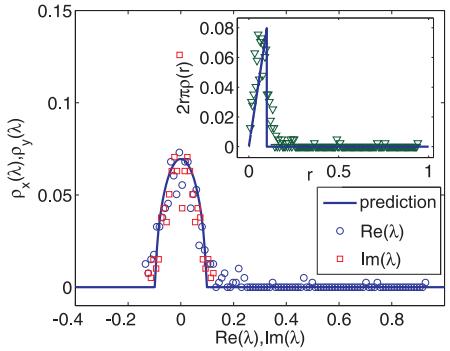

Fig. 4. Projection of the empirical spectrum pertaining to Fig. 3(c) on the real and imaginary axis [9]. The line is the analytical solution discussed in Section 2. The inset shows the empirical distribution of $\rho(|\lambda|)$ compared with the analytical analogue $2r\pi\rho(r)$.

at $\mathrm{Re}(\lambda) = 1$. Given the modest eigenvalue statistics ($N_\lambda = 400$) and the significant deviations outside the theoretical support, the agreement between the theoretical predictions for Gaussian noise and the bulk of the empirical data is rather satisfying.

4. Conclusion

We applied random matrix theory to lagged cross-correlation matrices and theoretically derived the eigenvalue spectra emanating from the respective real asymmetric random matrices in dependence of the information to noise ratio, Q. Specifically, we have shown that in the case of any eigenvalue 'gas' satisfying circular symmetry an inverse Abel-transform can be used to reconstruct the radial density, $\rho(r)$, from rescaled projections of the symmetrized problem. Based on these theoretical results we showed eigenvalue spectra associated to empirical cross-correlations of 5 min returns of the S&P500. For the full time-period observed, we found remarkable deviations, unambiguously demonstrating the inadequacy of the efficient market hypothesis at short time-scales.

We thank Z. Burda for a kind invitation to Cracow. We acknowledge support from the Austrian Science Fund under FWF projects P17621-G05 and P19132. C.B. would like to thank J.-P. Bouchaud for most valuable suggestions.

REFERENCES

[1] E.P. Wigner, *Ann. Math.* **62**, 548 (1955); *Ann. Math.* **67**, 325 (1958).

[2] J. Ginibre, *J. Math. Phys.* **6**, 440 (1965).

[3] N. Lehmann, H.-J. Sommers, *Phys. Rev. Lett.* **67**, 941 (1991).

[4] A. Edelman, *J. Multivariate Anal.* **60**, 203 (1997).

[5] E. Kanzieper, G. Akemann, *Phys. Rev. Lett.* **95**, 230201 (2005).

[6] J. Wishart, *Biometrika* **A20**, 32 (1928).

[7] K.B.K. Mayya, R.E. Amritkar, `cond-mat/0601279`.

[8] Z. Burda, A. Jarosz, J. Jurkiewicz, M.A. Nowak, G. Papp, I. Zahed, `cond-mat/0603024`.

[9] C. Biely, S. Thurner, *Quantitative Finance*, in print (2007).

[10] R.A. Janik, M.A. Nowak, G. Papp, J. Wambach, I. Zahed, *Phys. Rev.* **E55**, 4100 (1997).

[11] H.-J. Sommers, A. Crisanti, H. Somopolinsky, Y. Stein, *Phys. Rev. Lett.* **60**, 1895 (1988).

[12] V.L. Girko, *Spectral Theory of Random Matrices*, Nauka, Moscow, 1988.

[13] J.-P. Bouchaud, private communication, 2006.

[14] P.J. Forrester, `www.ms.unimelb.edu.au/ matpjf/matpjf.html`

[15] R. Bracewell, *The Fourier Transform and Its Applications*, McGraw-Hill, New York, 1965.

[16] J. Feinberg, R. Scalettar, A. Zee, *J. Math. Phys.* **42**, 5718 (2001).

[17] L. Laloux, P. Cizeau, J.-P. Bouchaud, M. Potters, *Phys. Rev. Lett.* **83**, 1467 (1999).

[18] V. Plerou, P. Goprikrishnan, B. Rosenow, L.A.N. Amaral, H.E. Stanley, *Phys. Rev. Lett.* **83**, 1471 (1999).

[19] M. Potters, J.-P. Bouchaud, L. Laloux, *Acta Phys. Pol. B* **36**, 9 (2005).